

Experimental Studies of a New Compact Design Four-Bed PSA Equipment for Producing Oxygen

Li Zhou, Jie Li, Wei Su, and Yan Sun

High Pressure Adsorption Laboratory (State Key Laboratory of Chemical Engineering), School of Chemical Engineering and Technology, Tianjin University, Tianjin 300072, China

Yaping Zhou

Dept. of Chemistry, School of Science, Tianjin University, Tianjin 300072, China

DOI 10.1002/aic.10508

Published online June 22, 2005 in Wiley InterScience (www.interscience.wiley.com).

A new compact design of pressure swing adsorption (PSA) equipment was presented. All columns of the PSA process reduced to disks that are stacked tightly together. The total size of the equipment was thus substantially reduced. The feasibility and the process performance of the new design were tested with a four-bed process aiming to produce oxygen from air. The adsorbent used was zeolite molecular sieve ZMS-5A. Although the process performance was limited by the relatively nonefficient adsorbent, the feasibility of the compact arrangement of disk columns was proven, and the advantages in the compensation of the thermal effect of adsorption and in the higher energy efficiency were also demonstrated. © 2005 American Institute of Chemical Engineers *AIChE J*, 51: 2695–2701, 2005

Keywords: PSA equipment, compact design, disk column, oxygen

Introduction

Sometimes there is a limitation on the dimension of pressure swing adsorption (PSA) equipment. For example, a continuous and convenient oxygen supply is important for a vehicle driven by hydrogen fuel cells for the normal delivery of the motor's power. However, the stringent space of the vehicle demands that the oxygen supplier must be compact. Oxygen producers for health care in hospitals or families must also be handy and compact. Such a task was usually performed by canned oxygen of different pressures; however, miniature PSA equipment has recently appeared in the market, and PSA technology of producing oxygen from air has matured in its development.^{1–4} However, even the latest patent⁵ of the miniature oxygen producer still follows the normal pattern of shape and arrangement of columns, as shown in Figure 1a. The clearance between the cylinder columns limits the further decrease of the

general size of the equipment. Therefore, a new compact PSA design, according to the principle shown in Figure 1b, was recently developed. Each column in the process reduces to a disk, and all disks are tightly stacked one above the other. Because the general dimension of multicolumn PSA equipment is basically controlled by the size and location of the columns, the new design will certainly reduce the total size of the equipment. To test the feasibility of the new design, PSA operations were carried out on a four-bed apparatus aiming to enrich oxygen from air.

Experimental Setup

The disks are made of stainless steel. The dimension of a disk is $88 \times 10 \times 10$ mm (OD \times wall thickness \times height), as shown in Figure 2. The adsorbent fills only the inner square part; therefore, the adsorbent volume in each disk is $48 \times 48 \times 10$ mm³. The gas inlet and outlet were put on the center of the opposite arcs. Small granular beads and fiber materials filled the arc area to function as the gas stream distributor or solid filter, whereas the two side arcs were blinded. The experimen-

Correspondence concerning this article should be addressed to L. Zhou at zhouli@tju.edu.cn.

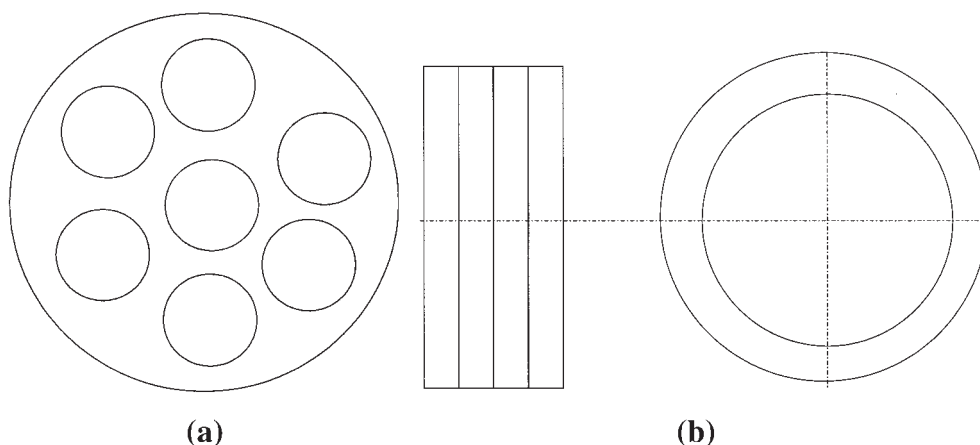


Figure 1. (a) Principal arrangement of cylinder columns in the latest patent of miniature PSA equipment. (b) Presented design of columns in a PSA equipment.

tal flowsheet is shown in Figure 3, and the step sequence in an operation cycle is shown in Table 1. A zeolite molecular sieve ZMS-5A (Shanghai Elegant Molecular Sieve Co. Ltd.) was used as the adsorbent. It was heated to 350–420°C for 3 h before filling in the disks. Adsorption isotherms of N₂ and O₂ on the adsorbent shown in Figure 4 were collected by a volumetric method. A residual gas analyzer (model QMS-100, Stanford Instrument) was used for on-line analysis of the gas stream composition. To determine an appropriate operation

condition, breakthrough curves (one of them is shown in Figure 5 as an example) were collected in situ on the experimental setup. The experiments were carried out first for a constant adsorption pressure and different feeding rates, and then for a constant feeding rate but different adsorption pressures. The condition of operating the four-bed PSA process was first determined, and then the process performance of the new design was examined under the selected condition.

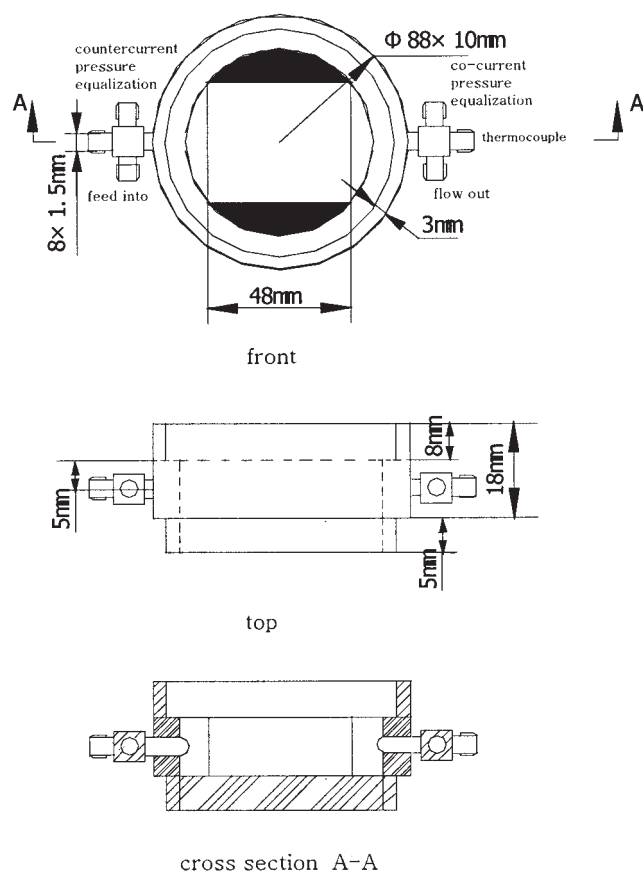


Figure 2. Dimension of a column disk.

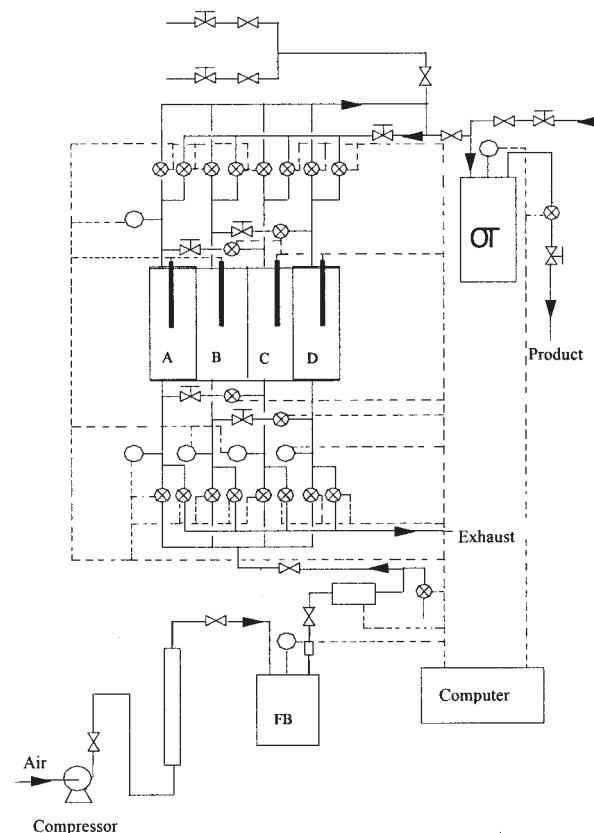


Figure 3. Experimental flowsheet.

—◇—, Valve; —◇—, Needle; —◇—, Solenoid. PS, pressure transducer; FB, feed buffer; OT, product tank; A, B, C, and D, disk columns; T, thermocouple; MFC, mass flow controller.

Table 1. Operation Plan of the Test Process*

I	A	PE	BD	PG	I	PE	RP
II	PE	BD	PG	I	PE	RP	A
III	PG	I	PE	RP	A	PE	BD
IV	PE	RP	A	PE	BD	PG	I

*A, adsorption; PE, pressure equalization; BD, blow down; PG, purge; I, idle; RP, repressurization.

Determination of Operation Condition

Adsorption pressure and feeding rate

Adsorption pressure and the feeding rate are the most important conditions for operating a PSA process. Their effect on process performance was examined by collecting breakthrough curves under the condition of either constant pressure or constant flow rate. The obtained breakthrough times are shown in Figure 6. It is seen from curve b that pressures > 0.6 MPa increase the breakthrough time only slightly, and thus 0.6 MPa was selected as the adsorption pressure. Similarly, 269.70 sccm (standard cubic centimeters per minute) was selected as the flow rate of the feed stream. The process performance was tested under the as-selected condition.

Environmental temperature

Environmental temperature exerts a substantial effect on process performance of the four-bed equipment, as shown in Figures 7 and 8. The experiments were carried out during winter and thus the room temperature was maintained at 18.5°C for subsequent experiments.

Purging ratio (P/F)

Purging the adsorbent bed with a stream of product can further desorb the adsorbed nitrogen and clear up the void space of the particle bed. The quantity of the purging steam is quantified as purging ratio: $P/F = \text{Quantity of the desired component in the purging stream} / \text{Quantity of the desired component in the feed stream}$.⁶ The effect of P/F on the concentration and recovery of

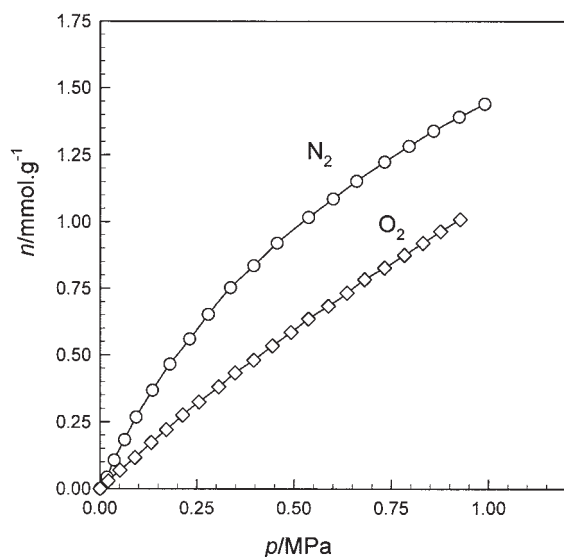


Figure 4. Adsorption isotherms of N_2 and O_2 on ZMS-5A at 298.15 K.

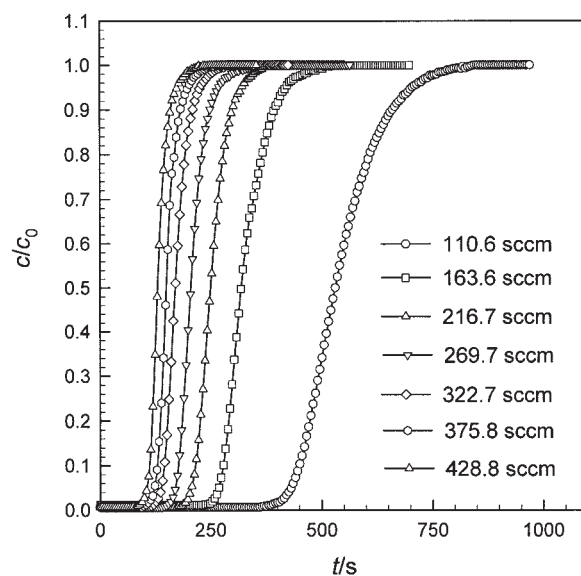


Figure 5. Breakthrough curves of the raw gas on ZMS-5A at adsorption pressure of 0.6 MPa and different feeding rates.

oxygen is shown in Figure 9. A proper value of P/F is selected on a trade-off basis between the product concentration and recovery, and 0.10 was selected for the present study.

The time allocated to each step of a cycle

Time of Adsorption (t_A). The time for the adsorption step should be less than the breakthrough time, yet still leave time for regulation. Because the pressure-equalization step follows the adsorption step, the duration of adsorption may affect the concentration and the recovery of product. Practically, different concentrations of oxygen are required for different applications. Therefore, to test the versatility of the equipment, different adsorption times were planned for different adsorption

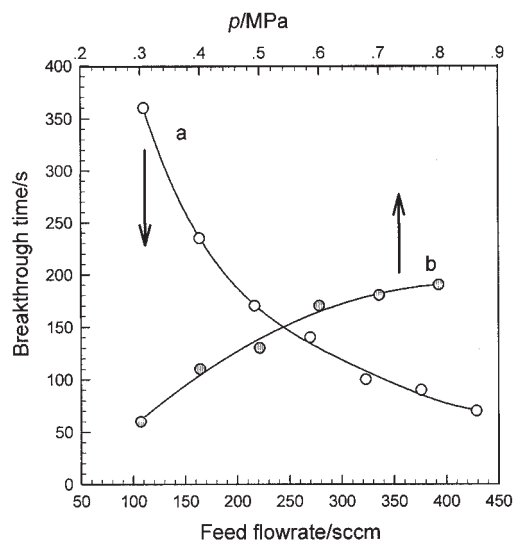


Figure 6. Breakthrough times at different feeding rates and adsorption pressures.

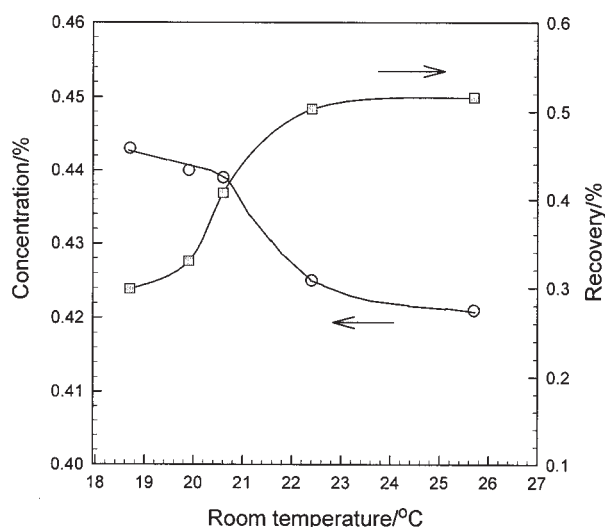


Figure 7. Influence of the environmental temperature on product concentration and recovery.

pressures, as shown in Table 2. The shortest time for each pressure is the lower limit of the adsorption step, below which the four-bed process cannot run normally.

Time of Blow Down (t_{BD}). The blow-down step follows the step of pressure equalization between a pair of columns. The duration of the blow-down step is the time needed for the adsorbed nitrogen to be desorbed; therefore, it affects the extent of regeneration of adsorbents. Different adsorption pressures may require different blow-down times; therefore, the appropriate time of blowing down was measured for each adsorption pressure, and the results were 20, 25, and 30 s for adsorption pressures 0.4, 0.5, and 0.6 MPa, respectively. The difference between them is negligible for the conditions tested. Therefore, 30 s was chosen as the blow-down time for all adsorption pressures in experiments.

Time for Pressure Equalization (t_{PE}). To increase recovery, as well as to recover part of the mechanical energy, the

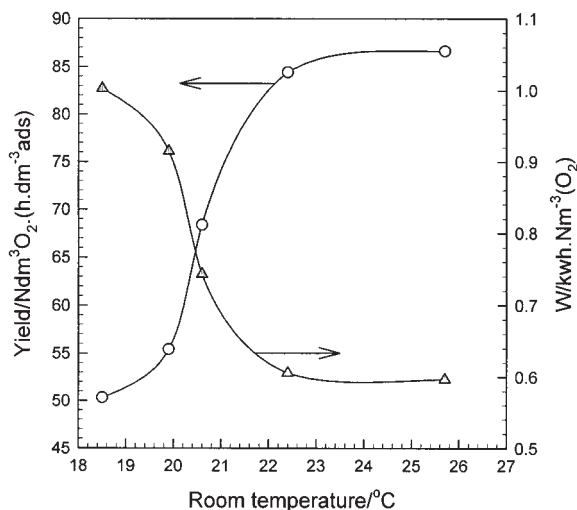


Figure 8. Influence of the environmental temperature on yield and energy consumption.

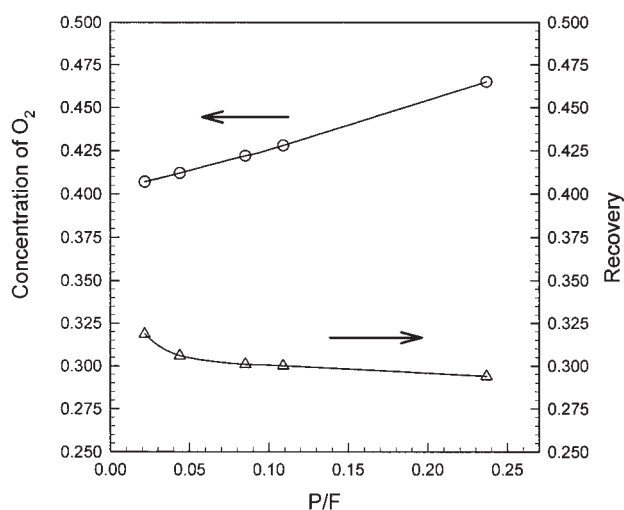


Figure 9. Influence of P/F on the concentration and recovery of O_2 for the cocurrent mode of pressure equalization.

step of pressure equalization is usually included in a PSA cycle. There are two modes of pressure equalization: equalization at the entrance ends (countercurrent pressure equalization) or equalization at the exit ends (cocurrent pressure equalization). The difference between the two modes of pressure equalization was also investigated. It was found that the difference did not affect the optimal time of each operation step, although cocurrent pressure equalization yielded better process performance than countercurrent pressure equalization, as shown in Table 3. Therefore, subsequent discussion is based on the use of the cocurrent pressure equalization mode. Although the time of pressure equalization scarcely affects energy consumption, it conversely affects the product concentration and recovery. Because product concentration is more sensitive than recovery to the variation of the equalization time (as shown in Figure 10), a shorter time—5 s—was adopted as the duration of the pressure-equalization step. However, the maximal gas speed at this step must not violate the speed limitation⁷ to keep the adsorbent bed stable.

Time of Purging (t_{PG}). The appropriate time of purging is determined by desorption dynamics and flow regime in the granular bed for a given quantity of purging stream. The effect of purging time on the concentration and recovery of oxygen is shown in Figure 11. There is a maximum of oxygen concentration at 6 s, whereas the recovery is not very sensitive to the purging time; therefore, the purging time is selected as 6 s.

Time of Repressurization (t_{RP}). Repressurization with the product stream follows the step of pressure equalization to reach the pressure of adsorption in the regenerated column. As shown in Figure 12, the time of repressurization hardly affects the concentration or recovery of oxygen, but does affect the

Table 2. Adsorption Times for Different Adsorption Pressures

Adsorption pressure, MPa	0.4	0.5	0.6
Duration of the adsorption step, s	80, 70, 60	100, 80, 70	120, 100, 90, 80

Table 3. Effect of Pressure Equalization Mode on Process Performance

Mode of Pressure Equalization	Pressure of Adsorption (MPa)	Time of Adsorption (s)	Time of Repressurizations	Oxygen Concentration	Oxygen Recovery
Cocurrent	0.6	120	110	0.443	0.300
Countercurrent	0.6	120	110	0.417	0.272
Cocurrent	0.5	80	70	0.553	0.262
Countercurrent	0.5	80	70	0.475	0.215
Cocurrent	0.4	80	70	0.414	0.270
Countercurrent	0.4	80	70	0.394	0.211

stability of the product tank pressure, as shown in Figure 13. Therefore, the time of repressurization is preferred to be longer, but it has to meet the following constraint:

$$t_{RP} = \begin{cases} t_A - t_{pg} & t_{pg} \geq t_{PE} \\ t_A - t_{PE} & t_{pg} < t_{PE} \end{cases} \quad (1)$$

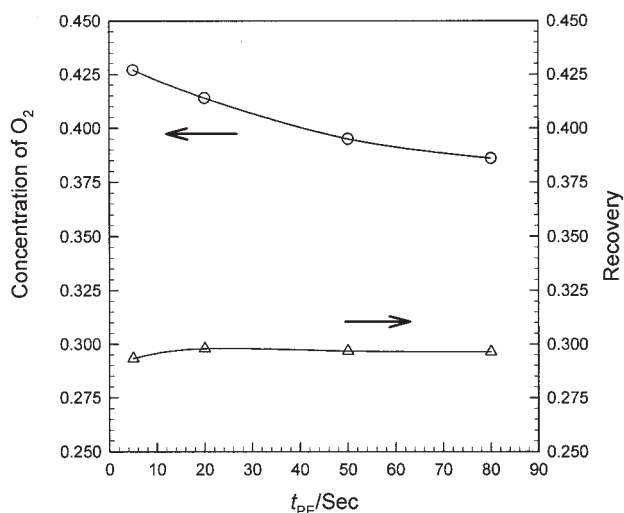


Figure 10. Influence of t_{PE} on the concentration and recovery of O_2 .

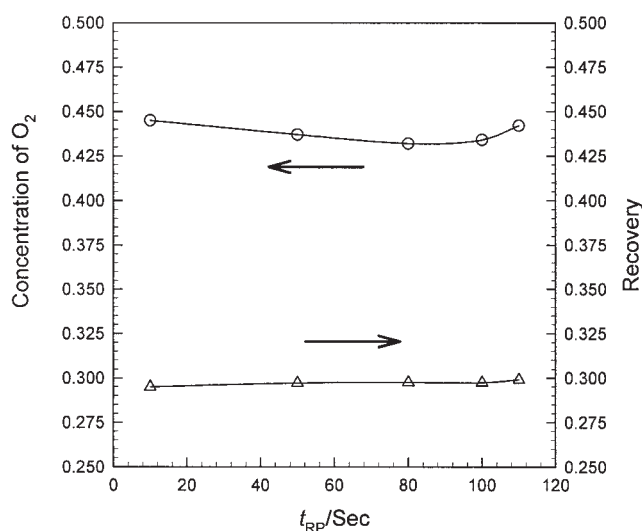


Figure 12. Influence of t_{RP} on the concentration and recovery of O_2 .

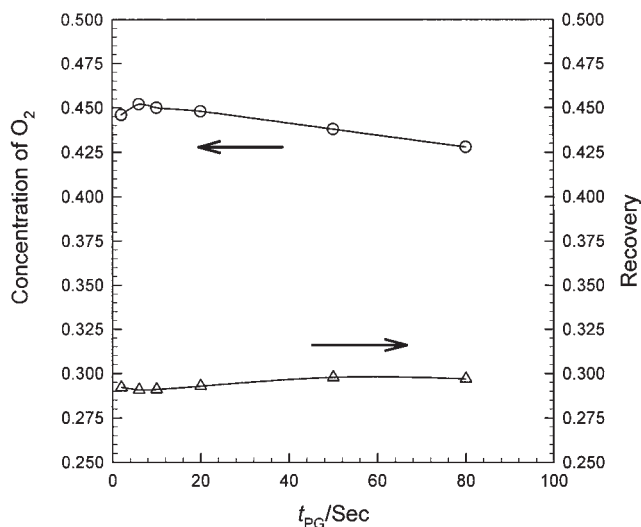


Figure 11. Influence of t_{pg} on the concentration and recovery of O_2 .

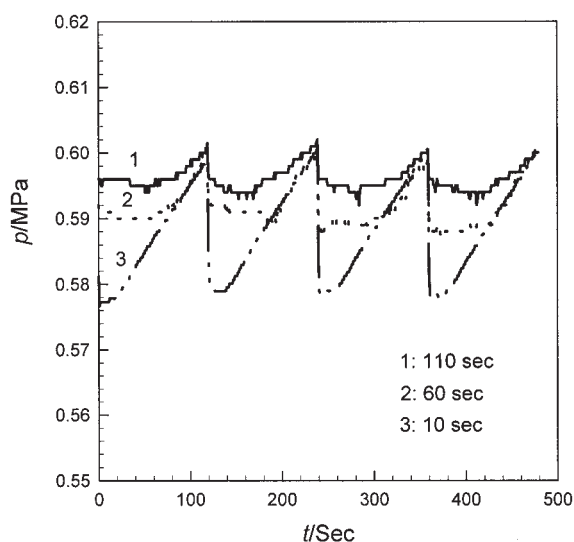


Figure 13. Influence of t_{RP} on the pressure fluctuation of the product tank within an operation cycle.

Table 4. Operation Condition of the Cyclic Process

Column	t_A (s)	t_{BD} (s)	t_{PE} (s)	P/F	t_{PG} (s)	t_{RP} (s)
A, B, C, or D	Adjustable	30	5	0.1	6	Varied with t_A

adsorption pressure and time on process performance, and the operation stability in multiple cycles were studied for the as-determined operation condition and cycling sequence.

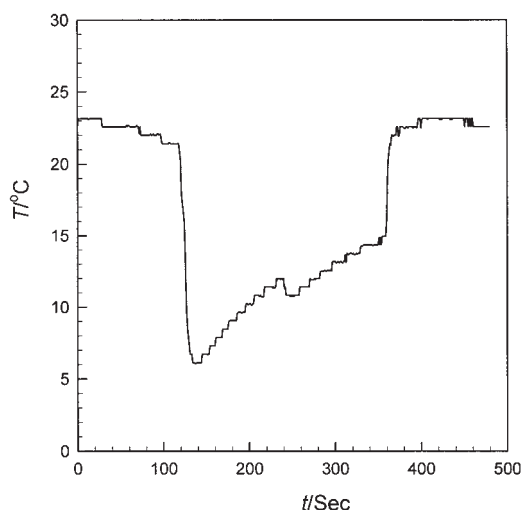
Process Performance

Variation of column temperature in an operation cycle

A T-type thermocouple was inserted into the center of each disk column to monitor the variation of bed temperature during an operation cycle. Typical temperature variation in a single column is shown in Figure 14 for the following conditions (using cocurrent pressure equalization): adsorption pressure, 0.6 MPa; adsorption time, 120 s; repressurization time, 110 s; flow rate of the feed stream, 269.7 sccm. The temperature variation in the adsorption step is $<4^\circ\text{C}$. The relatively small increase in bed temperature is favorable for an adsorption process. The bed temperature decreased $<15^\circ\text{C}$ during pressure equalization and blowing-down operations. The temperature varied about $2\text{--}3^\circ\text{C}$ during purging. The total temperature variation during a cycle is reasonable; therefore, the thermal effect of adsorption only slightly affects the separation process. As shown in Table 5, if one column is in adsorption, its neighbor column must be in desorption. Therefore, the thermal effect of adsorption has thus been partially compensated. This might be an additional advantage of the compact arrangement of disk columns.

Process performance under different adsorption conditions

The process performance under different pressures and times of adsorption is summarized in Table 6. The oxygen concentration is in the 44.3–71% range, which satisfies the requirement of health-care applications.⁸ Oxygen recovery is between 15.3 and 30% for 18.5°C . However, the oxygen concentration decreases to 42.1% as the temperature increases to 25.7°C , although the recovery increases considerably from 30 to 51.6%. The energy consumption for the above-mentioned concentration range is between 0.8 and $1.97\text{ kWh/Nm}^3\text{O}_2$ at 18.5°C . The energy consumption decreased from 1.00 to $0.59\text{ kWh/Nm}^3\text{O}_2$ as the temperature increased to 25.7°C . The average energy consumption of miniature oxygen producers is about $1.5\text{ kWh/Nm}^3\text{O}_2$, and the best set might be as low as $0.5\text{--}0.6\text{ kWh/Nm}^3\text{O}_2$. The energy efficiency of the compact

**Figure 14. Temperature variation of a column within an operation cycle.**

design equipment is rather high considering the adsorbent used is not the best choice. Oxygen recovery would be considerably increased, and the energy consumption level will substantially decrease if an adsorbent of much better selectivity is used.

Operation stability

To test the operation stability of the new design, 150 cycles (a cycle lasts for 6 min) were continuously run for the following conditions (using the cocurrent pressure equalization mode): feed flow rate, 269.7 sccm; adsorption pressure, 0.6 MPa; adsorption time, 90 s; pressure equalization time, 5 s; blow-down time, 30 s; $P/F = 0.1$; purging time, 6 s; repressurization time, 80 s. Variation of the oxygen concentration and recovery with the number of cycles is shown in Figure 15. The operation started at cycle 0, and the pressure of the product tank was 0.1 MPa, which was gradually increased to 0.6 MPa at cycle 11 when the product stream began to release. The totally stable state was reached at cycle 81, and the oxygen concentration fixed at 63.9% and the recovery fixed at 24.0%.

Discussion and Conclusions

(1) Although the new PSA design is operable, the performance is moderate. The major reason is the efficiency of the adsorbent used was not high. It is well known that the enrichment of oxygen using zeolite molecular sieves is based on the difference between O_2 and N_2 in the equilibrium adsorption. Molecular sieve ZMS-5A is one of the earliest adsorbents used for enrichment.

Table 5. Final Operation Plan of the Process*

A			PE ↑	BD ↓	I	PG ↓	I		PE ↓	I	RP ↓
PE ↑	BD ↓	I	PG ↓	I		PE ↓	I	RP ↓	A		
PG ↓		I	PE ↓	I	RP ↓	A			PE ↑	BD ↓	I
PE ↓	I	RP ↓	A			PE ↑	PD ↓	I	PG ↓	I	

*I, idle; ↑, cocurrent flow; ↓, countercurrent flow; otherwise, terms are the same as in Table 1.

Table 6. Process Performance for Different Adsorption Pressures and Times at 18.5°C

Adsorption Pressure (MPa)	Adsorption Time (s)	Oxygen Concentration	Oxygen Recovery	Output per Unit Volume of Adsorbent (NLO ₂ /hL)	Energy Consumption (kWh/Nm ³ O ₂)
0.6	120	0.443	0.300	50.3	1.003
0.6	100	0.545	0.290	48.7	1.037
0.6	90	0.639	0.240	40.2	1.255
0.6	80	0.71	0.153	25.6	1.970
0.5	100	0.437	0.295	49.5	0.916
0.5	80	0.553	0.262	43.9	1.032
0.5	70	0.651	0.168	28.2	1.607
0.4	80	0.414	0.270	45.3	0.862
0.4	70	0.466	0.261	43.8	0.890
0.4	60	0.576	0.249	41.7	0.936

However, the one we had is not an efficient species for enriching oxygen from air. The separation factor evaluated from the breakthrough curves is only around 2.0 for the pressure range tested. We tried to modify the adsorbent, although improvement was not achieved. Some other efficient adsorbent was also tried, but humidity was strongly adsorbed, thus causing some trouble in dealing with it. ZMS-5A was finally used in the performance test because of the time limit for the student. Although not efficient, it can maintain a stable operation. If a better adsorbent could be used, however, better performance of the new design would be more clearly demonstrated.

(2) In addition to the reduction of the general equipment size, higher energy efficiency is a prominent feature of the new PSA design because part of the thermal effect of adsorption could be compensated for by the thermal effect of desorption. This advantage could be more prominent on further improving

the design of step sequence and using better heat-transfer material to separate the disk-type beds.

(3) The PSA operation process can be well simulated with a two-dimensional model for the disk-type beds. The plug-flow regime could be established more closely in the adsorbent bed, and higher efficiency of mass transfer could be expected.

(4) The new PSA design does not change the nature of separation, and can be applied for processes of either equilibrium or kinetically controlled separation systems.

(5) It is concluded that the new PSA design provides a possibility of constructing small but efficient oxygen-producing equipment, which may have important implications for fuel cell-driven vehicles and health-care applications.

Acknowledgments

This work is supported by The Natural Science Foundation of China (Grants 20276049 and 20336020).

Literature Cited

1. Yang RT. *Gas Separation by Adsorption Processes*. London: Butterworths; 1987.
2. Ruthven DM, Farooq S, Knaebel KS. *Pressure Swing Adsorption*. New York, NY: VCH; 1994.
3. Sircar S, Kratz WC. A pressure swing adsorption process for production of 23–50% oxygen-enriched air. *Sep Sci Technol*. 1988;23:437–450.
4. Yoshida S, Ogawa N, Kamioka K, Hirano S, Mori T. Study of zeolite molecular sieves for production of oxygen by using pressure swing adsorption. *Adsorption*. 1999;5:57–61.
5. U.S. Patent No 6 068 680. Rapid cycle pressure swing adsorption oxygen concentration method and apparatus; May 30, 2000.
6. Yang RT, Doong SJ. Gas separation by pressure swing adsorption: A pore-diffusion model for bulk separation. *AIChE J*. 1985;31:1829–1842.
7. White DH Jr, Barkley PG. The design of pressure swing adsorption systems. *Chem Eng Prog*. 1989;85:25–33.
8. Yang YL, Lu ZH. A discussion on the oxygen concentration of a PSA producer for health care application (in Chinese). *Technol Deep Cryogen*. 1996;4:24–25.

Manuscript received Jun. 21, 2004, and revision received Jan. 15, 2005.

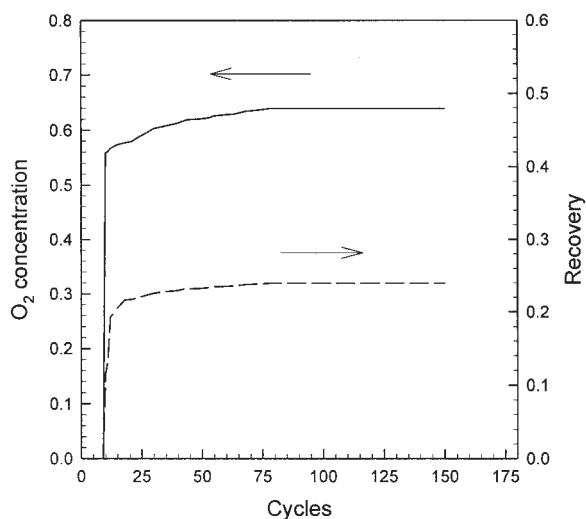


Figure 15. Variation of the oxygen concentration and recovery in multicycle runs.